

Supporting Information

**Initial-stage oriented-attachment one-dimensional assembly of nanocrystals:
Fundamental insight with a collision-recrystallization model**

Yu Pan,^{1†} Weiqiang Lv,^{1†} Yinghua Niu,¹ Kechun Wen,¹ Xiaorong Hou,¹ Jianmin Gu,¹ Minda Zou,¹
Luhan Ye,¹ Wei Wang,² Kelvin HL Zhang,^{3*} Weidong He^{1,4,5*}

¹ School of Energy Science and Engineering, University of Electronic Science and Technology of China (UESTC), Chengdu 611731, PR China, ² School of Materials Science and Engineering, Shenzhen Graduate School, Harbin Institute Technology, Shenzhen 518055, PR China, ³ Department of Materials Science & Metallurgy, University of Cambridge, 27 Charles Babbage Road, Cambridge, UK CB3 0FS, ⁴ Interdisciplinary Program in Materials Science, Vanderbilt University, Nashville, Tennessee 37234-0106, USA, ⁵ Vanderbilt Institute of Nanoscale Science and Engineering, Vanderbilt University, Nashville, Tennessee 37234-0106, USA. Correspondence and requests for materials should be addressed to K.H.L. Zhang and W. He. (Emails: hz256@cam.ac.uk, weidong.he@uestc.edu.cn and weidong.he@vanderbilt.edu). †These two authors contribute equally to this work.

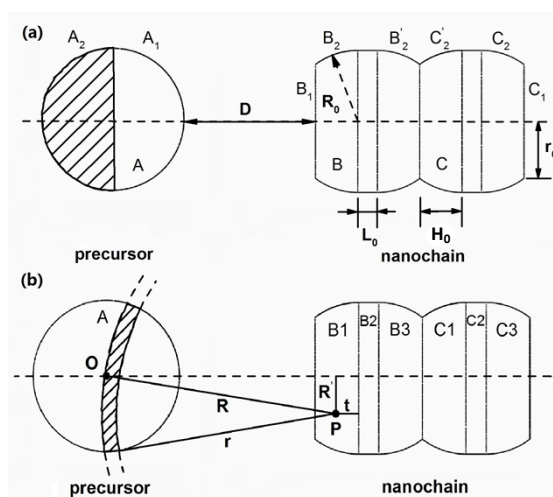


Figure S1. Configuration of the approaching spherical precursor and the growing nanochain: (a) illustration of geometrical parameters in the derivation of the geometric relations and the EDL interaction, (b) illustration of geometrical parameters for the derivation of the vdW interaction.

Derivation of the geometric relations

As shown in Figure S1a, the correlation between these two radii can be expressed in Eq. S1,

$$r_0 = \left(R_0^2 - H_0^2 \right)^{1/2} \quad (\text{S1})$$

where H_0 is the thickness of the nanochain spherical segment. r_0 and R_0 the radii of two side surfaces of the spherical segment, respectively.

In our model, it is assumed that the nanochain maintains a fixed volume and a fixed radius in the evolution of the nanochain to nanorod. So, the volume identity can be given is Eq. S2,

$$\pi R_0^2 L_0 + \frac{1}{3} \pi H_0 (3R_0^2 + 3r_0^2 + H_0^2) = \frac{4}{3} \pi R_0^3 \quad (\text{S2})$$

where L_0 is the length of the cylindrical part in the nanochain.

Simplifying Eq. S2, we obtain the expression of the length L_0 in Eq. S3.

$$L_0 = \frac{4R_0^3 - 6H_0R_0^2 + 2H_0^3}{3R_0^2} \quad (S3)$$

Curve fitting of the temperature dependence of surface potential

The surface potential ψ_0 of the nanoparticles can be determined by the Nernst equation as shown in Eq. S4,¹

$$\psi_0 = \frac{k_B T}{xe} \ln\left(\frac{c}{c_{zp}}\right) \quad (S4)$$

where k_B is the Boltzmann constant, e is the elementary charge, T represents the temperature of the solution, x is the valence number of the potential-determining ions M^{x+} , c is the concentration of the potential-determining ions M^{x+} , and c_{zp} is denoted as p.z.c. (point of zero charge). c_{zp} is expressed as the form of negative decimal logarithm in Eq. S5.

$$pM_{pzc} = -\log(c_{zp}) \quad (S5)$$

The correlation between the pM_{pzc} and the temperature can be deduced from the Gibbs-Helmholtz equation as shown in Eq. S6,^{2,3}

$$2R \ln(10) \left(\frac{1}{2} pL - pM_{pzc} \right) = \frac{\Delta H^*}{T} - \Delta S^* \quad (S6)$$

where pL is the negative decimal logarithm of the solubility product of the potential-determining ions, R is the ideal gas constant, and ΔH^* and ΔS^* are the standard differential enthalpy and the standard differential entropy of ions transfer, respectively.

The temperature dependence of the pL of silver iodide has been measured in experiments by Lyklema, as shown in Table 1.²

Temperature (K)	pL
278	17.20
288	16.32
298	15.73
308	15.13
318	14.61
328	14.06
338	13.59
348	13.12
358	12.69

For obtaining the expression of the temperature dependence of pL , the curve fitting is applied. Fitted by the rational function with one numerator degree and one denominator degree, the correlation between the pL and the temperature is shown in Eq. S7.

$$pL = \frac{1.267T + 3191}{T - 71.41} \quad (S7)$$

The coefficient of determination of this curve fitting R^2 is equal to 0.9992 indicating that the curve fits well the experiment data.

By substituting Eqs. S5, S6 and S7 into Eq. S4, the temperature dependence of ψ_0 is shown in Eq. S8,

$$\psi_0 = \frac{k_B T}{e} \left[\ln(c_0) + \frac{\ln(10)}{2} \frac{1.267T + 3191}{T - 71.41} - \frac{1}{2R} \left(\frac{\Delta H^*}{T} - \Delta S^* \right) \right] \quad (S8)$$

where $\Delta H^* = 76.82$ kJ/Mol, $\Delta S^* = 175.30$ J/Mol·K for silver iodide, and $c_0 = 1.333 \times 10^{-5}$ Mol/L by assuming $\psi_0 = 50$ mV at 298 K.

Derivation of the EDL interaction between the growing nanochain and spherical precursor NC

The EDL interaction energy per unit area between two infinite flat surfaces is given by Eq. S9,¹

$$E(h) = 64k_B T n_\infty \kappa^{-1} \Upsilon_0^2 \exp(-\kappa h) \quad (S9)$$

where n_∞ is the concentration of indifferent ions far from nanoparticles and h is the separation between two infinite flat surfaces. For the $z : z$ supporting electrolyte, the Debye–Hückel length κ^{-1} is given in Eq. S10,¹

$$\kappa = \left(\frac{2z^2 e^2 n_\infty}{\varepsilon k_B T} \right)^{1/2} \quad (S10)$$

where ε represents the absolute permittivity of the solution. The parameter Υ_0 is expressed as Eq. S11.¹

$$\Upsilon_0 = \frac{\exp(ze\psi_0 / 2k_B T) - 1}{\exp(ze\psi_0 / 2k_B T) + 1} \quad (S11)$$

Hereby, the EDL interaction between curved surfaces by the surface element integration (SEI) is shown in Eq. S12,⁴

$$U_{EDL} = \int_{S_1} dU = \int_{A_1} \mathbf{n}_2 \cdot \mathbf{k}_2 \frac{\mathbf{n}_1 \cdot \mathbf{k}_1}{|\mathbf{n}_1 \cdot \mathbf{k}_1|} E(h) dA_1 \quad (S12)$$

where \mathbf{n}_1 and \mathbf{n}_2 are the unit normal vectors outward the approximated surface, \mathbf{k}_1 and \mathbf{k}_2 are the unit vectors which are parallel with the respective z axes, and dA_1 is the infinitesimal projected area of the surface element dS_1 .

As shown in Figure 1a, the total EDL interaction can be viewed as the superposition of two parts of interaction: the forward hemispherical facet A_1 of the precursor with the nanochain BC and the backward one A_2 with the nanochain BC, as given in Eq. S13.

$$U_{EDL} = U_{EDL}^{A_1 BC} + U_{EDL}^{A_2 BC} \quad (S13)$$

The EDL interaction between the hemispherical facet A_1 and the nanochain BC can be divided further into six subdivisions as shown in Eq. S14.

$$U_{EDL}^{A_1 BC} = U_{EDL}^{A_1 B_1} + U_{EDL}^{A_1 B_2} + U_{EDL}^{A_1 B_2'} + U_{EDL}^{A_1 C_2} + U_{EDL}^{A_1 C_2'} + U_{EDL}^{A_1 C_1} \quad (S14)$$

These six EDL interactions are figured out in the cylindrical coordinate as follows,

$$U_{EDL}^{A_1 B_1} = \int_0^{r_0} E(R_0 + D - \sqrt{R_0^2 - r^2}) 2\pi r dr \quad (S15)$$

$$U_{EDL}^{A_1 B_2} = \int_{r_0}^{R_0} \sqrt{1 - (r/R_0)^2} E(R_0 + D + H_0 - 2\sqrt{R_0^2 - r^2}) 2\pi r dr \quad (S16)$$

$$U_{EDL}^{A_1B_2'} = \int_{r_0}^{R_0} -\sqrt{1-(r/R_0)^2} E(R_0 + D + H_0 + L_0) 2\pi r dr \quad (S17)$$

$$U_{EDL}^{A_1C_2'} = \int_{r_0}^{R_0} \sqrt{1-(r/R_0)^2} E(R_0 + D + 3H_0 + L_0 - 2\sqrt{R_0^2 - r^2}) 2\pi r dr \quad (S18)$$

$$U_{EDL}^{A_1C_2} = \int_{r_0}^{R_0} -\sqrt{1-(r/R_0)^2} E(R_0 + D + 3H_0 + 2L_0) 2\pi r dr \quad (S19)$$

$$U_{EDL}^{A_1C_1} = \int_0^{r_0} -E(R_0 + D + 4H_0 + 2L_0 - \sqrt{R_0^2 - r^2}) 2\pi r dr \quad (S20)$$

where D is the minimum separation between the precursor and the nanochain. Furthermore, the term

$\mathbf{n}_2 \cdot \mathbf{k}_2 \frac{\mathbf{n}_1 \cdot \mathbf{k}_1}{|\mathbf{n}_1 \cdot \mathbf{k}_1|}$ is equal to ± 1 for flat surfaces or $\pm \sqrt{1-(r/R_0)^2}$ for spherical surfaces. Similarly, the

EDL interaction between the hemispherical facet A_2 and nanochain BC can also be divided into six subdivisions as shown in Eq. S21.

$$U_{EDL}^{A_2BC} = U_{EDL}^{A_2B_1} + U_{EDL}^{A_2B_2} + U_{EDL}^{A_2B_2'} + U_{EDL}^{A_2C_2'} + U_{EDL}^{A_2C_2} + U_{EDL}^{A_2C_1} \quad (S21)$$

These six EDL interactions are computed in the cylindrical coordinate as follows.

$$U_{EDL}^{A_2B_1} = \int_0^{r_0} -E(R_0 + D + \sqrt{R_0^2 - r^2}) 2\pi r dr \quad (S22)$$

$$U_{EDL}^{A_2B_2} = \int_{r_0}^{R_0} -\sqrt{1-(r/R_0)^2} E(R_0 + D + H_0) 2\pi r dr \quad (S23)$$

$$U_{EDL}^{A_2B_2'} = \int_{r_0}^{R_0} \sqrt{1-(r/R_0)^2} E(R_0 + D + H_0 + L_0 + 2\sqrt{R_0^2 - r^2}) 2\pi r dr \quad (S24)$$

$$U_{EDL}^{A_2C_2'} = \int_{r_0}^{R_0} -\sqrt{1-(r/R_0)^2} E(R_0 + D + 3H_0 + L_0) 2\pi r dr \quad (S25)$$

$$U_{EDL}^{A_2C_2} = \int_{r_0}^{R_0} \sqrt{1-(r/R_0)^2} E(R_0 + D + 3H_0 + 2L_0 + 2\sqrt{R_0^2 - r^2}) 2\pi r dr \quad (S26)$$

$$U_{EDL}^{A_2C_1} = \int_0^{r_0} E(R_0 + D + 4H_0 + 2L_0 + \sqrt{R_0^2 - r^2}) 2\pi r dr \quad (S27)$$

Derivation of the vdW interaction between the growing nanochain and spherical precursor NC

The vdW interaction energy between two macroscopic bodies is shown in Eq. S28,⁵

$$U_{vdW} = - \int_{V_1} dv_1 \int_{V_2} dv_2 \frac{q^2 \lambda}{r^6} \quad (S28)$$

where dv_1 and dv_2 are both the volume elements of macroscopic particles, V_1 and V_2 are the particle volumes, q is expressed as the atom density of the interactional particles, λ is defined as London-van der Waals constant, and r represents the separation between dv_1 and dv_2 . As shown in Figure 1b, the vdW interaction between the precursor and an atom of point P in the nanochain E_p can be written as Eq. S29.

$$E_p = - \int_{R-R_0}^{R+R_0} \frac{\pi \lambda q}{r^5 R} [R_0^2 - (R-r)^2] dr \quad (S29)$$

The integration result of Eq. S29 is given in Eq. S30.

$$E_p = -\frac{4\pi\lambda qR_0^3}{3(R^2 - R_0^2)^3} \quad (\text{S30})$$

If we integrate qE_p (point P) throughout the domain of one spherical segment of the nanochain, the vdW interaction between this spherical segment and the spherical precursor is given in Eq. S31.

$$U_{vdW} = -\int_0^{H_0} dt \int_0^{\sqrt{R_0^2 - t^2}} qE_p \cdot 2\pi R' dR' \quad (\text{S31})$$

If we integrate qE_p throughout the domain of one cylindrical part of the nanochain, the vdW interaction between this cylindrical part and the spherical precursor is shown in Eq. S32.

$$U_{vdW} = -\int_0^{L_0} dl \int_0^{R_0} qE_p \cdot 2\pi R' dR' \quad (\text{S32})$$

In general, the constant $\pi^2 q^2 \lambda$ before the integration is substituted by the Hamaker constant A . Therefore, the vdW interactions between the precursor with the four spherical segments and two cylindrical parts are expressed as follows.

$$U_{vdW}^{AB1} = -\frac{8}{3} A \int_0^{H_0} dl \int_0^{\sqrt{R_0^2 - l^2}} \frac{R_0^3 R'}{[R'^2 + (R_0 + D + H_0 + l)^2 - R_0^2]^3} dR' \quad (\text{S33})$$

$$U_{vdW}^{AB2} = -\frac{8}{3} A \int_0^{L_0} dl \int_0^{R_0} \frac{R_0^3 R'}{[R'^2 + (R_0 + D + H_0 + l)^2 - R_0^2]^3} dR' \quad (\text{S34})$$

$$U_{vdW}^{AB3} = -\frac{8}{3} A \int_0^{H_0} dt \int_0^{\sqrt{R_0^2 - t^2}} \frac{R_0^3 R'}{[R'^2 + (R_0 + D + H_0 + L_0 + t)^2 - R_0^2]^3} dR' \quad (\text{S35})$$

$$U_{vdW}^{AC1} = -\frac{8}{3} A \int_0^{H_0} dt \int_0^{\sqrt{R_0^2 - t^2}} \frac{R_0^3 R'}{[R'^2 + (R_0 + D + 3H_0 + L_0 - t)^2 - R_0^2]^3} dR' \quad (\text{S36})$$

$$U_{vdW}^{AC2} = -\frac{8}{3} A \int_0^{L_0} dl \int_0^{R_0} \frac{R_0^3 R'}{[R'^2 + (R_0 + D + 3H_0 + L_0 + l)^2 - R_0^2]^3} dR' \quad (\text{S37})$$

$$U_{vdW}^{AC3} = -\frac{8}{3} A \int_0^{H_0} dt \int_0^{\sqrt{R_0^2 - t^2}} \frac{R_0^3 R'}{[R'^2 + (R_0 + D + 3H_0 + 2L_0 + t)^2 - R_0^2]^3} dR' \quad (\text{S38})$$

The total vdW interaction is the sum of these six parts, which is shown in Eq. S39.

$$U_{vdW} = U_{vdW}^{AB} + U_{vdW}^{AC} = U_{vdW}^{AB1} + U_{vdW}^{AB2} + U_{vdW}^{AB3} + U_{vdW}^{AC1} + U_{vdW}^{AC2} + U_{vdW}^{AC3} \quad (\text{S39})$$

Reference

1. Hiemenz, P. C.; Rajagopalan, R. *Principles of Colloid and Surface Chemistry, revised and expanded*; CRC Press, 1997; Vol. 14.
2. Berube, Y.; de Bruyn, P. L. *Journal of Colloid and Interface Science* **1968**, *27*, 305.
3. Lopez Valdivieso, A.; Reyes Bahena, J.; Song, S.; Herrera Urbina, R. *Journal of colloid and interface science* **2006**, *298*, 1.
4. Bhattacharjee, S.; Elimelech, M.; Borkovec, M. *Croat. Chem. Acta* **1998**, *71*, 883.
5. Hamaker, H. *physica* **1937**, *4*, 1058.